J. Geogr. Sci. 2020, 30(6): 988-1004
DOI: https://doi.org/10.1007/s11442-020-1766-z

Simulation and construction of the glacier mass balance in the Manas River Basin, Tianshan, China from 2000 to 2016

ZHAO Guining[1], *ZHANG Zhengyong[1], LIU Lin[1], LI Zhongqin[1,2], WANG Puyu[2], XU Liping[1]

1. College of Sciences, Shihezi University, Shihezi 832000, Xinjiang, China;
2. State Key Laboratory of Cryospheric Science, Northwest Institute of Eco-Environment and Resources, CAS, Lanzhou 730000, China

Abstract: The glacier mass balance (GMB) is an important link between climate and water resources and has remarkable regulatory functions in river runoff. To simulate changes of the GMB and to analyze the recharge rates of glacier meltwater to runoff in the Manas River Basin (MRB) during 2000–2016, MOD11C3, TRMM 3B43 and other multi-source remote sensing data were used to drive the degree-day model. The results showed that: (1) the accuracy of the remote sensing meteorological data can be corrected effectively by constructing the temperature and precipitation inversion models, and the characteristics of glacial climate can be finely described through downscaling. The average annual temperature was –7.57 °C and the annual precipitation was 410.71 mm in the glacier area of the MRB. The zone at an altitude of about 4200 m was a severe climate change zone, and above and below that zone, the temperature drop rates were –0.03°C/100 m and –0.57°C/100 m, respectively, while precipitation gradients were –2.66 mm/100 m and 4.89 mm/100 m, respectively. (2) The overall GMB was negative with a cumulative GMB of up to –9811.19 mm w.e. and the average annual GMB fluctuated between –464.85 and –632.19 mm w.e. Besides, the glacier melted slowly during 2000–2002 and 2008–2010, but rapidly for 2002–2008 and 2010–2016, while the most serious loss of the glacier occurred in 2005–2009. Moreover, the vertical changes of the GMB increased at 244.83 mm w.e./100 m in the ablation zone but only at 18.77 mm w.e./100 m in the accumulation zone. (3) The intraannual runoff strongly responded to the change of the GMB especially in July and August when the loss of the GMB accounted for 75.4% of the annual loss, and when runoff accounted for 55.1% of the annual total. Due to differences in the annual precipitation and snow meltwater outside the glacier, the interannual glacier meltwater recharge rates fluctuated between 19% and 31%. The recharge rate of glacier meltwater to runoff in the MRB was close to that for other basins in the Tianshan Mountains, which may be used as a basis to confirm the reliability of the estimated GMB results. Furthermore, based on the present findings, it is recommended that the research community pursue studies on the GMB in other alpine river basins.

Keywords: multi-source remote sensing data; degree-day model; glacier mass balance (GMB); glacial meltwater; Manas River Basin (MRB)

Received: 2019-12-10 **Accepted:** 2020-02-09
Foundation: National Natural Science Foundation of China, No.41761108, No.41771077
Author: Zhao Guining, Master, specialized in response of glaciers to climate change. E-mail: 13345492733@163.com
***Corresponding author:** Zhang Zhengyong, PhD, E-mail: zyz0815@163.com

1 Introduction

Against a background of global warming, glaciers as "solid reservoirs" are being strongly affected by climate change. While mountain glaciers located in mid-low latitudes are more sensitive to climate change (Li *et al.*, 2019), the glacier mass balance (GMB) is not only an indicator of regional climate change but also the mass basis of runoff change (Naegeli *et al.*, 2019). Direct measurement is one of the usual methods to study specific changes of the GMB using marking poles and snow pits. Given the complexity of glacial topography, direct observation is very difficult and thus simulation models of the GMB may be effective; in this context a physical model of energy balance and the degree-day model to describe the water balance are used widely (Cascone *et al.*, 2019). Given the complexity and the difficulty in acquiring model parameters, the energy-mass balance model is generally limited to a single glacier using a detailed series of measured data, while the degree-day model is widely used on a larger scale due to its simplicity and strong universality. Many studies have shown that the degree-day model can achieve similar results as the energy-mass balance model at the watershed-scale (Wang *et al*., 2019). In addition, temperature and precipitation data for the degree-day model generally come from the surrounding meteorological stations or auto-meteorological instruments that are laid out in the glacier area, such that spatial interpolation methods with temperature lapse rates and precipitation gradients are obtained. However, such methods ignore the effect of differences in terrain on the climate (Smid *et al.*, 2018). Although temperature and precipitation data are readily available by spatial interpolation methods, these data are generally considered to be low in objectivity and fineness, and this traditional method of obtaining meteorological data limits the degree of accuracy that can be obtained in glacier mass balance simulations (Mackay *et al*., 2018). Meanwhile, with application of remote sensing technology in meteorological monitoring, various kinds of remote sensing products are used in meteorological forecasting and services. Given the good retrieval effect with respect to snow and ice temperatures, MOD11C3 data is very suitable for high altitude areas at middle latitudes (Song *et al.*, 2016; Michaelides *et al.*, 2017). Also, precipitation data of TRMM 3B43 are widely used to recalculate the defined precipitation information in complex geographical regions (Zhu *et al.*, 2017; Cao *et al.*, 2018). Therefore, remote sensing meteorological data, such as MOD11C3 and TRMM 3B43, can provide a new way to obtain meteorological data in alpine glacier regions and overcome the limitations of the observed meteorological data. However, the lower spatial resolution of the remote sensing data cannot meet the input requirements of the degree-day model, therefore, it is necessary to improve the resolution of MOD11C3 and TRMM 3B43 data via downscaling methods (Ezzine *et al.*, 2017). To reflect the particular changes of the GMB, glacier meltwater is often introduced and regarded as a product of the GMB such that it has a profound impact on regional water resources.

Glacier meltwater in the Tianshan Mountains plays a supporting role in oasis economic development and ecological construction. At present, the studies of the GMB in the Tianshan Mountains are not limited to typical glaciers (Zhang *et al*., 2019). To analyze the temporal and spatial distribution patterns and changes of the GMB, many researchers have tried to carry out simulations in regions where the GMB research is extremely scarce (Kronenberg *et al*., 2016; Wang *et al*., 2019). The Manas River originates from the northern slopes of the Tianshan Mountains, and its runoff plays a decisive role in agricultural development of the

Shihezi reclamation regions in the lower reaches (Wang *et al*., 2017). However, changes of the GMB are rarely discussed in the Manas River Basin (MRB). In this study, MOD11C3 and TRMM 3B43 data were used to characterize the distribution of temperature and precipitation in the glacier area, and to drive the degree-day model to simulate changes of the GMB, and calculate the recharge rates of glacier meltwater to runoff. Our findings may provide a reference and useful information for management and utilization of water resources in the MRB.

2 Study area

The MRB (43°27'–45°21'N, 85°01'–86°32'E), located in the southern Dzungaria Basin of the northern Tianshan Mountains (Figure 1). The basin has a typical continental climate with an average annual temperature of 6–6.9℃ and annual precipitation of 110–200 mm (Xu *et al*., 2019). According to the *Concise Glacier Inventory of China*, more than 800 glaciers are distributed among the upper reaches of the Manas River, with the largest being in the Junggar Basin with an area of 608.25 km^2 (Shi, 2009). The runoff dissipating district is below the outlet, and the confluence area is from the outlet to altitudes of about 1500 m; the main runoff producing area is between 1500 and 3600 m, and regions over 3600 m are covered by snow throughout the year. The Kenswat Hydrological Station, the outlet control station of the Manas River, is at an altitude of about 900 m (Li *et al*., 2012).

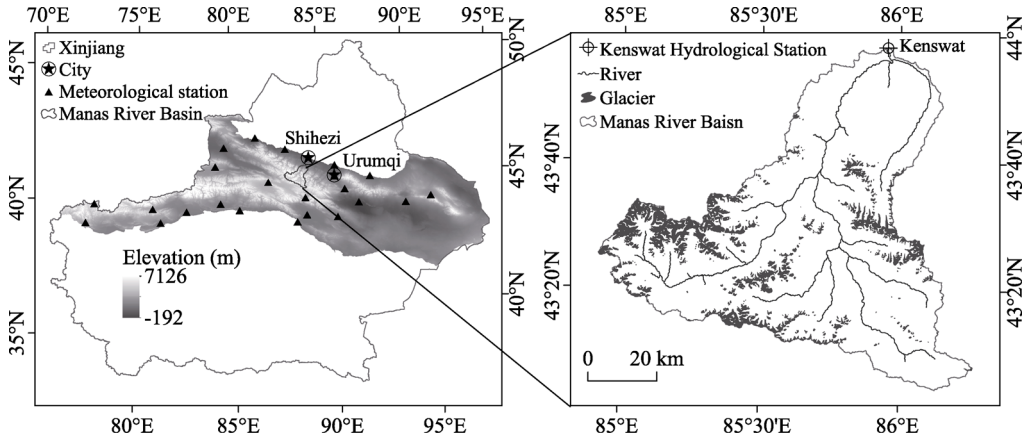

Figure 1 Location of the Manas River Basin

3 Data and methods

3.1 Data

The data include mainly multi-source remote sensing data and measured meteorological and hydrological data (Table 1). The Digital Elevation Model (DEM) was used to divide the glacier area into elevation zones, in order to extract terrain factors used for inversion models of temperature and precipitation, such as slope and aspect. MOD11C3 and TRMM 3B43 data were used to describe the spatial distribution of temperature and precipitation in the mountain area. The Normalized Difference Vegetation Index (NDVI) reflects vegetation coverage.

Measured meteorological data were used to verify the accuracy of the inversion results and the applicability of the inversion model. Measured hydrological data were used to analyze the variation characteristics of runoff in the Manas River and verify the simulation accuracy of the glacier meltwater. The data on glacier area were derived from the Second Glacier Inventory Dataset of China that was compiled in the middle term of our study period. Snow density data were used to calculate the snow degree-day factors of the glacier.

Table 1 Data sources

Category	Time	Resolution	Official website
NDVI	2000–2016	250 m × 250 m	NASA (https://www.nasa.gov/)
MOD11C3		0.05° × 0.05°	
TRMM 3B43		0.25° × 0.25°	
DEM	2010	30 m × 30 m	Geospatial Data Cloud (http://www.gscloud.cn/)
Temperature	2000–2016		National Meteorological Information Center (http://data.cma.cn/)
Precipitation			
Glacier area	2006–2010		Scientific Data Center for Cold and Arid Regions (http://westdc.westgis.ac.cn/)
Snow density	2014		Document (Chen *et al.*, 2015)
Runoff	2000–2016		Kenswat Hydrological Station

3.2 Methods

The downscaled inversion MOD11C3 and TRMM 3B43 data were used to run the degree-day model to simulate the GMB in the MRB from 2000 to 2016. First, the inversion models between the measured and the remote sensing meteorological data were constructed with other terrain impact factors to improve the accuracy of the temperature and precipitation data for the Tianshan Mountains. Second, the temperature and precipitation inversion data were downscaled by DEM data to a resolution of 30 m × 30 m. Then, the recalculated meteorological data were evaluated using the Root Mean Square Error (RMSE) and coefficient of determination (R^2) values. Finally, MOD11C3 and TRMM 3B43 data that met the requirements of precision and resolution were input into the degree-day model to simulate change of the GMB in the MRB.

3.2.1 Construction of temperature and precipitation inversion models

Climate factors play a decisive role in the change of the GMB. However, the complex geographical environment in alpine areas restricts effective long-term climate monitoring. To describe climate characteristics objectively in the glacier area, MOD11C3 and TRMM 3B43 data were used to replace the traditional monitoring meteorological data. Due to the limitations of the topography or the sensors, remote sensing meteorological products are prone to problems such as “high-value underestimation” or “low-value overestimation” (Cao *et al*., 2018), which results in specific errors in the actual meteorological values. Previous studies have shown that the distribution patterns of temperature and precipitation are affected by factors such as geographic location, altitude, slope, aspect and the underlying surface as reflected by the NDVI (Mcpartland *et al*., 2019). Therefore, based on the correlation of geographic factors and the remote sensing data and the measured meteorological data, inversion models of temperature and precipitation were constructed to improve the accuracy of

MOD11C3 and TRMM 3B43.

There is only one national meteorological station (Shihezi) located close to the study area. Ideally, to achieve accuracy in the inversion models, the study range should be expanded to include the 23 meteorological stations in the Tianshan Mountains. The monthly temperature and precipitation regression models were established between the monthly multi-source remote sensing data and the monthly measured meteorological data (Equation 1). The monthly coefficients for the regression model are shown in Tables 2 and 3, and the RMSE and R^2 values were used to evaluate the applicability of the inversion models and the accuracy of the recalculated temperature and precipitation inversion values. The RMSE can give a measure of the degree of dispersion between the inversion and the measured data, and R^2 can reflect their correlation. Thus the smaller the RMSE and the larger the R^2 values are, the stronger is the applicability of the inversion models and the higher the accuracy of the inversion results. The monthly average temperature regression models (Table 2) show that the RMSE values were in the range 1.15–3.06 and the R^2 values were greater than 0.89, which indicates that the degree of dispersion between the inversion and measured temperature values was low and their correlation was high, reflecting strong applicability and high accuracy of the average monthly temperature inversion models in the Tianshan Mountains. From the monthly precipitation regression models (Table 3), the RMSE values were slightly larger, fluctuating between 3.69 and 19.69, which show that the degree of dispersion between inversion and measured precipitation values was relatively high. The R^2 values were in the range 0.71–0.88, which indicates a good correlation, thus the monthly precipitation inversion models have good applicability and the precipitation inversion values can accurately depict the actual distribution of precipitation in the mountain areas. The comprehensive evaluation results for temperature and precipitation inversion data reflect the fact that the inversion of remote sensing meteorological data can accurately and objectively describe the climate characteristics in the Tianshan Mountains. The governing equation for the model is

$$y = \lambda + ax_1 + bx_2 + cx_3 + dx_4 + ex_5 + fx_6 + gx_7 \quad (1)$$

where y is the measured temperature or precipitation, λ is the intercept, x_1 is the latitude, x_2 is the longitude, x_3 is the altitude, x_4 is the slope, x_5 is the aspect, x_6 is the NDVI, x_7 is MOD11C3 or TRMM 3B43. The terms a, b, c, d, e, f and g are regression coefficients.

Although it is believed that remote sensing meteorological data can objectively depict the climate characteristics in mountainous regions, the basin-scale simulation of the GMB still cannot meet input requirements of the degree-day model. Generally, further downscaling methods may be used to improve the spatial resolution of remote sensing data to achieve fine detail of the local climate (Zhang *et al*., 2017; Zhang *et al*., 2018). Therefore, based on the inversion models of temperature and precipitation in the Tianshan Mountains, the DEM with a resolution of 30 m × 30 m was used as the standard for downscaling to obtain the temperature and precipitation data for each elevation zone in the study area. The detailed methodology for downscaling is described elsewhere (Jia *et al*., 2011).

3.2.2 Description of the degree-day model

For glacier and snow melting, the amount of melting in a certain period is given by (Zhang *et al*., 2012)

Table 2 Coefficients and accuracy of the monthly temperature regression model

Month	Regression factor coefficient								Accuracy	
	λ	a	b	c	d	e	f	g	RMSE	R^2
1	5.41	1.12	–0.64	–0.0020	0.210	0.0110	3.89	1.57	3.06	0.89
2	56.48	–0.47	–0.41	–0.0040	0.260	0.0101	8.97	1.38	1.78	0.94
3	121.38	–2.05	–0.26	–0.0070	0.220	0.0130	15.43	1.22	2.88	0.95
4	143.06	–2.54	–0.11	–0.0120	0.170	0.0060	6.88	0.84	1.82	0.94
5	140.79	–2.31	–0.05	–0.0100	0.170	0.0043	–1.61	0.76	1.16	0.95
6	127.95	–1.80	–0.04	–0.0130	0.136	0.0080	–4.57	0.63	1.16	0.96
7	108.19	–1.36	–0.04	–0.0130	0.120	0.0120	–5.25	0.66	1.42	0.96
8	109.65	–1.40	–0.05	–0.0130	0.120	0.0110	–5.25	0.63	1.16	0.94
9	111.77	–1.70	–0.04	–0.0090	0.160	0.0101	–3.00	0.72	1.30	0.92
10	81.19	–1.35	–0.10	–0.0058	0.208	0.0058	6.03	1.06	1.15	0.89
11	48.80	–0.57	–0.25	–0.0034	0.240	0.0110	9.49	1.18	1.27	0.90
12	51.62	0.26	–0.71	–0.0030	0.280	0.0120	–14.49	0.62	1.52	0.90

Table 3 Coefficients and accuracy of the monthly precipitation regression model

Month	Regression factor coefficient								Accuracy	
	λ	a	b	c	d	e	f	g	RMSE	R^2
1	19.27	–1.15	0.34	–0.0021	0.049	0.0036	–1.86	1.15	3.69	0.74
2	42.42	–2.33	0.68	–0.0030	0.136	–0.0020	–38.85	1.18	9.31	0.76
3	–60.87	1.32	0.04	–0.0018	–0.006	0.0105	4.37	1.03	6.75	0.81
4	158.81	–4.82	0.65	–0.0113	0.108	0.0011	–29.9	1.64	10.33	0.85
5	63.84	–2.64	0.66	–0.0053	0.065	–0.0054	–24.15	1.31	13.20	0.85
6	–149.02	2.60	0.44	0.0095	–0.014	–0.0289	–19.10	1.01	14.41	0.88
7	–174.73	2.97	0.47	0.0145	0.106	–0.0261	–11.22	0.97	14.33	0.83
8	–83.76	1.29	0.26	0.0113	0.072	–0.0201	–11.61	1.11	19.69	0.84
9	–25.69	1.09	–0.27	0.0001	–0.027	0.0172	–20.52	1.51	8.43	0.82
10	38.29	0.60	–0.72	–0.0034	0.038	0.0143	–8.00	0.91	8.42	0.85
11	60.39	–1.92	0.28	–0.0047	0.035	–0.0002	–5.51	1.12	9.08	0.78
12	–4.97	–0.06	0.10	–0.0024	0.001	0.0007	–6.95	0.93	4.29	0.71

$$A = D \times PDD \tag{2}$$

where A is the melt water equivalent of glacier ice and snow in a certain period (mm w.e), D is the degree-day factor of glacier ice/snow (mm/(℃·d)), and PDD is the cumulative positive temperature in a certain period (℃), which can be obtained by (Zhang *et al.*, 2012):

$$PDD = \int_{N_1-1}^{N_2} \frac{1}{\delta\sqrt{2\pi}} \int_0^{+\infty} T_m e^{\frac{-(T_m-T_a)^2}{2\delta^2}} d_T d_t \tag{3}$$

where T_m (℃) is the average monthly temperature and presents a normal distribution over the year, T_a is the average yearly temperature (℃), δ is the standard deviation of the temperature distribution, N_1 and N_2 are the start and end dates for the calculation and the time

interval is $N = N_2 - N_1 + 1$.

The net GMB at a certain point (or altitude) (Zhang *et al*., 2012) is

$$B_i = P + A + f \tag{4}$$

where B_i is the GMB (mm w.e.) in a certain period, P is glacier surface accumulation by solid precipitation (mm w.e.) in a certain period, A is glacier ablation (mm w.e.), and f is glacier meltwater refreezing rate or internal replenishment (mm w.e.) usually calculated as 10% of the amount melted (Zhang *et al.*, 2006).

Solid precipitation can be calculated by the double critical temperature method (Van *et al.*, 2010)

$$P_S = \begin{cases} P & T \leqslant T_S \\ \dfrac{T_L - T}{T_L - T_S} & T_S < T < T_L \\ 0 & T \geqslant T_L \end{cases} \tag{5}$$

$$P_L = P - P_S \tag{6}$$

where P_S and P_L are the solid and liquid precipitation (mm), P is the total monthly precipitation (mm), T is the average monthly temperature (℃), T_S and T_L are the critical temperatures of solid and liquid precipitation (℃), taken as –0.5℃ and 2℃, respectively, and determined according to the observation data of the Urumqi glacier No.1 in the Tianshan Mountains (Zhang *et al.*, 2006).

The GMB of the entire glacier is (Zhang *et al.*, 2012)

$$B_n = \frac{1}{S}\sum\nolimits_i^n B_i S_i \tag{7}$$

where S_i is the glacier area of each glacier band (m^2), and glacial elevation is divided into 20 elevation bands from 3278 m to the glacial top in 100 m band thicknesses and with the entire glacier being calculated from all the elevation bands.

The degree-day factors, with clear spatial heterogeneity, and including the snow degree-day factor (D_s) and the ice degree-day factor (D_i), reflect the speed of melting of snow and ice at unit temperature in a day. Observation snow density data were collected (Chen *et al.*, 2015) and then the snow density for the whole study area was obtained by the kriging interpolation method. Finally, the snow degree-day factor for each elevation zone was counted using Equation 8 (Muattar *et al.*, 2016). However, the ice degree-day factor varies according to specific conditions such as elevation, slope, aspect and shading (Zhang *et al.*, 2006). Therefore, the ice degree-day factor for each elevation band was computed by Equation 9 (Chen, 2014).

$$D_s = 1.1 \times \frac{\rho_s}{\rho_w} \tag{8}$$

where D_s is the snow degree day factor (mm/(℃·d)), calculated from the snow density (ρ_s, kg/m^3) and the density of water (ρ_w, kg/m^3).

$$D_i = -105.7\varphi + 96.8\lambda + 0.03h - 0.8\cos(\omega - 180) + 20.3\sin\alpha - 3447.4 \tag{9}$$

where D_i is the ice degree-day factor (mm/(℃·d)), φ *is the* latitude (°), λ is the longitude (°), ω is the aspect (°), and α is the slope (°).

3.3 Accuracy verification

3.3.1 Glacier mass balance

With respect to the default for the measured or simulated data of the GMB in the MRB, historical documents on the Urumqi Glacier No.1 (Glacier No.1) and the Haxilegen Glacier No.51 of the Kuytun River (Glacier No.51) during the contemporaneous period were used. Glacier No.1 is 82 km to the east and Glacier No.51 is 108 km to the west of the MRB. These glaciers are often used as reference standards to test the reliability of the simulated GMB values in the MRB. As one of ten reference glaciers identified by the WGMS (World Glacier Monitoring Organization), Glacier No.1 is the longest and the most systematically monitored glacier in China. Glacier No.51, the second reference glacier fixed-point monitoring site at the Tianshan Glaciological Station of China, is also a typical glacier on the northern slope of the Tianshan Mountains and has been observed 1–2 times a year since 1998 (Wang *et al.*, 2016). Thus the measured GMB data of the above two glaciers can provide verification for the simulated GMB values in the MRB. In addition, Wu *et al.* (2011) used the degree-day model to simulate the long-series of the GMB in Glacier No.1, and whose results are very consistent with the measured values. Therefore, it is concluded that the accuracy of the simulated GMB in the MRB can be referred to the measured GMB values for Glaciers No.1 and No.51. The average GMB value in the MRB was –577.13 mm w.e./a from 2000 to 2016, while Mu *et al.* (2019) reported an average value of –677 mm w.e./a via observation of Glacier No.1 from 1996 to 2015. Also, Zhang *et al.* (2018) achieved a simulation for the GMB of –370 mm w.e./a in Glacier No.51 based on a temperature-index model from 1999 to 2015. It has been inferred that the GMB gaps may be related to westerly precipitation that continuously decreases from west to east in the Tianshan Mountains. If the glacier is closer to the west of the Tianshan Mountains, it would receive more precipitation and clearly the glacier would have a greater supply, thus the glacier deficit would be smaller; otherwise, the glacier deficit would be larger. Concurrently, the overall temperature rises from the west to the east in the Tianshan Mountains, which would also lead to stronger ablation of the glaciers. In general, the simulated results reflect the basic characteristics of the GMB in the MRB.

3.3.2 Glacier meltwater

Glacier meltwater is closely associated with changes of the GMB and can also be considered as an indicator to test the accuracy of the simulated GMB results in data-deficient regions. We estimated the amount of glacier meltwater and its recharge rate to river runoff each year (Table 4) and compared the values with the recharge rate of other rivers in the northern slopes of the Tianshan Mountains. The average recharge rate of glacier meltwater in the Junggar endorheic drainage area was reported as 27.13% (Lan *et al.*, 2007) and this is consistent with a value of 25% for the data in the present study. The recharge rate estimated by Yang (1987) at the Hongshanzui Hydrological Station in the MRB was 34.6%, a higher value than our results; it might be that the difference in the Hongshanzui data compared with the data at the Kenswat Hydrological Station is due to the lower altitude of Hongshanzui and the fact that the glacier area is relatively large (608.3 km^2). Although glacier thinning is weaker for a lower annual temperature than currently, the total amount of glacier meltwater is relatively large, and these influencing elements would cause a larger recharge rate of gla-

cier meltwater. The Kuytun River and the Urumqi River are all typical rivers supplied by ice and snow ablation on the northern slope of the Tianshan Mountains with their contribution rates to glacier meltwater being 29.4% (Shen *et al.*, 2013) and 26.7%, respectively (Sun *et al.*, 2017), which are also similar to the recharge rates of the Manas River. In comparison, the simulated recharge rate of the Manas River is accurate, which also means the GMB simulation results are reliable.

Table 4 The GMB, glacier meltwater and recharge rates in the MRB during 2000–2016

Year	ELA (m)	GMB (mm.w.e.)	Glacier meltwater (10^8 m^3)	River runoff (10^8 m^3)	Recharge rate of glacier meltwater
2000	4538	–545.86	3.29	16.29	0.20
2001	4550	–566.88	2.99	14.43	0.21
2002	4530	–551.41	3.51	18.74	0.19
2003	4558	–584.20	3.22	11.05	0.29
2004	4560	–620.49	3.47	12.28	0.28
2005	4532	–575.59	3.37	13.39	0.25
2006	4588	–632.19	3.63	13.18	0.28
2007	4537	–602.90	3.68	15.47	0.24
2008	4569	–624.72	3.27	13.77	0.24
2009	4507	–464.85	2.91	11.00	0.26
2010	4533	–527.05	3.36	16.62	0.20
2011	4560	–602.95	3.65	11.74	0.31
2012	4555	–597.01	3.46	12.54	0.28
2013	4553	–587.42	3.41	13.37	0.25
2014	4556	–563.95	3.21	10.65	0.30
2015	4573	–605.61	4.01	18.35	0.22
2016	4528	–558.11	3.48	15.45	0.23
Average	4549	–577.13	3.41	14.02	0.25

4 Results

4.1 Characteristics of temperature and precipitation

Glaciers are highly sensitive to climate change, but the complexity of glacial climate and the difficulty of comprehensive monitoring restricts accurate meteorological studies in alpine regions, thus in such circumstances the accuracy of the GMB simulation may be compromised. Hence, the inversion models of temperature and precipitation combined with downscaling methods were constructed to improve dramatically the accuracy of the meteorological data. During the period 2000–2016, the average interannual temperature of the glaciers in the MRB was –7.57℃ (Figures 2a and 2b). From the vertical changes of the GMB, the turnover point of temperature was at an altitude of about 4200 m because the temperature decreased at a relatively large rate of 0.57℃/100 m from the glacial terminal to 4200 m but then at a smaller rate of 0.03℃/100 m from 4200 m to 4700 m; thereafter, there was a sharp change between 4700 and 4800 m with a sudden drop of 1.48℃/100 m and finally a minimum of –8.85℃ was reached at 4800 m. The interannual average precipitation of the glaciers in the MRB was 410.71 mm and this also shifted significantly at 4200 m with a maxi-

mum of 418.25 mm; thereafter, precipitation increased at a rate of 4.89 mm/100 m from the glacier terminus to 4200 m but at a decreasing rate of 2.66 mm/100 m from 4200 m to 4700 m, then a minimum of 399.89 mm at 4700 m was reached and finally there was a rapid increase of 5.17 mm/100 m from 4700 m to the top of the glacier (Figures 2a and 2b).

Climate change is the key to variation of the GMB, especially in the melting period (May to September). It was observed that the changes of temperature and precipitation in the melting period (Figures 2c and 2d) were remarkably consistent with their annual periods (Figures 2a and 2b), thus indicating that the annual variations are deeply affected by the changes in the melting period. During the glacial ablating period, an altitude of 4200 m is the dividing line for changes of temperature and precipitation, the temperature lapse rate being –0.65℃/100 m below this point but being –0.17℃/100 m above 4200 m. The minimum temperature appears at an altitude of about 4800 m. The precipitation gradient below 4200 m, from 4200 m to 4800 m and from 4800 m to the top of the glacier is 5.9 mm/100 m, –2.04 mm/100 m and 6.24 mm/100 m, respectively. Moreover, the maximum precipitation zone lies in between 4100 and 4200 m in the MRB. In general, the meteorological inversion models combined with the downscaling methods can improve considerably the objectivity and performance of the MOD11C3 and TRMM 3B43 data in the MRB.

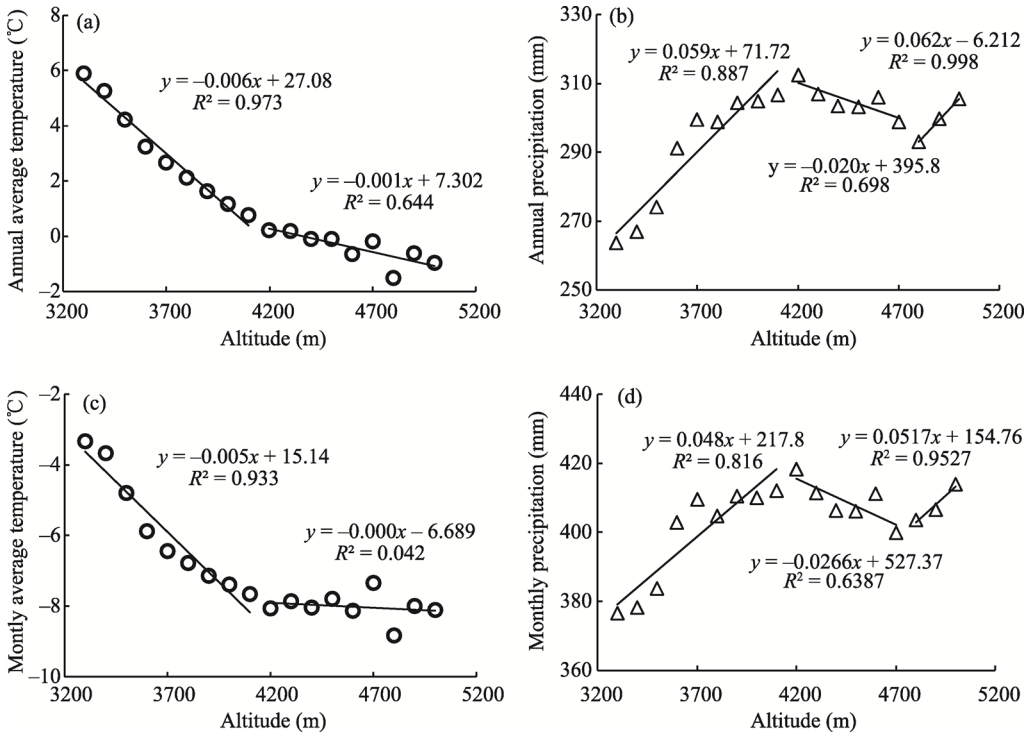

Figure 2 Annual average temperature and annual precipitation, and monthly average temperature and precipitation in the glacier ablation period for the Manas River Basin

4.2 Characteristics of the GMB change

The changes of the GMB, reflected in the sum of the glacier ablation and accumulation, continuously appeared negative in the MRB during the study period (Table 4). The accumu-

lated GMB was –9811.19 mm w.e. (–577.13 mm w.e./a), which is equivalent to a glacial thinning of 11 m (ice density of 0.9 kg/m^3). The minimum negative GMB was in 2009 (–464.85 mm w.e.), and the maximum negative GMB occurred in 2006 (–632.19 mm w.e.). The interannual variations of the GMB were expressed with the multi-year anomalies and cumulative anomalies of the GMB (Figure 3a). There were positive anomaly values during the 7 years, which indicated that glacial ablation was weak, while the anomalies of other years were negative implying that glacial ablation was strong. The cumulative anomalies demonstrated that glacial ablation slowed down during 2000–2002 and during 2008–2010 with rates of 17.98 mm w.e./a and 81.18 mm w.e./a, respectively, while glacial ablation intensified during 2002–2008 and 2010–2016 with rates of –29.55 mm w.e./a and –8.71 mm w.e./a, respectively. The cumulative GMB was below the average value during 2005–2009 with the strongest ablation occurring at this stage. The cumulative anomalies attained a minimum in 2008 (–110.08 mm w.e.) because anomalies were always below zero from 2003 to 2008. However, the continuous negative anomaly suddenly stopped in 2009, and this mutation phenomenon also occurred for Glacier No.1 (Zhang *et al.*, 2013). In terms of the intraannual variation of the GMB, the glacial accumulation period (October to April) lasted a long time but was not obvious (93.18 mm w.e.); it started in October but became most obvious in April of the following year when precipitation was significant (Figure 3b). Regarding the other months when accumulation occurred, though their temperatures were lower than that of April's, the amounts of precipitation were also less resulting in an entire weak accumulation. While the melting period was relatively short and the glacier mass loss was serious (–670.31 mm w.e.), the glacier began to show a deficit in early May and subsequently extended to the negative maximum of the GMB in August, however, the glacial melting slowed down with the drop in temperature. Within a year, the overall glacial warming and cooling processes were transformed greatly, which also made the intraannual changes of the GMB show features of "weak accumulation with strong ablation" in the MRB.

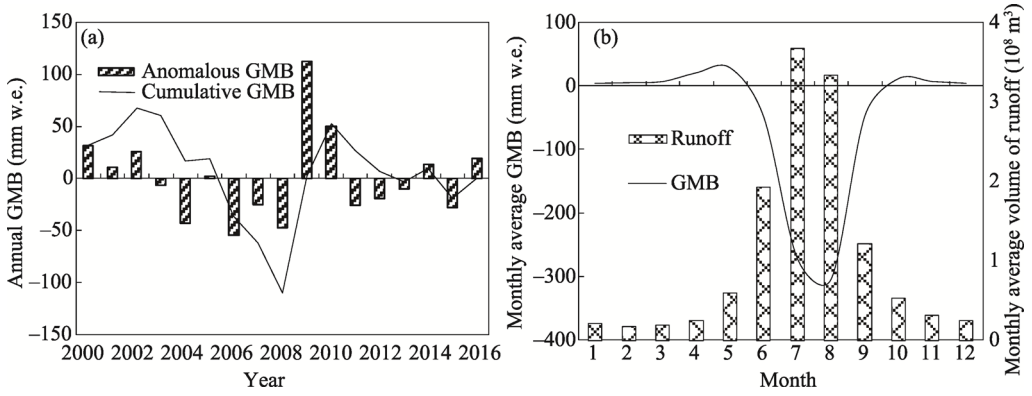

Figure 3 Interannual GMB anomalies with cumulative anomalies and the monthly GMB with runoff in the Manas River Basin

The GMB change also had significant vertical zonality because there were some differences of hydrothermal combination and degree-day factors in the elevation bands (Figure

4). The GMB for each elevation band indicated that it achieved a negative maximum (–3112.53 mm w.e.) in the terminal band of 3300–3400 m but gradually altered with rise in altitude to a positive value for the zone 4500–4600 m, and then it reached a positive maximum (283.24 mm w.e.) at the zone 4800–4900 m. Above 4900 m, the positive GMB decreased again because precipitation became less and the temperature rose above this altitude. The Equilibrium Line Altitude (ELA), a key index to reflect changes of the GMB, was calculated by the GMB in each elevation band. The positions of the ELA showed the final conditions of annual accumulation and ablation of the glaciers such that separation of "the above accumulation area" from "the below ablation area" was revealed. During the study period, the interannual ELA positions fluctuated between 4500 and 4600 m with an average altitude of 4549 m, the highest altitude (4588 m) occurred in 2006 and the lowest altitude (4057 m) appeared in 2009, which indicated that 2006 and 2009 were, respectively, the strongest and the weakest years for melting of the glaciers (Table 4).

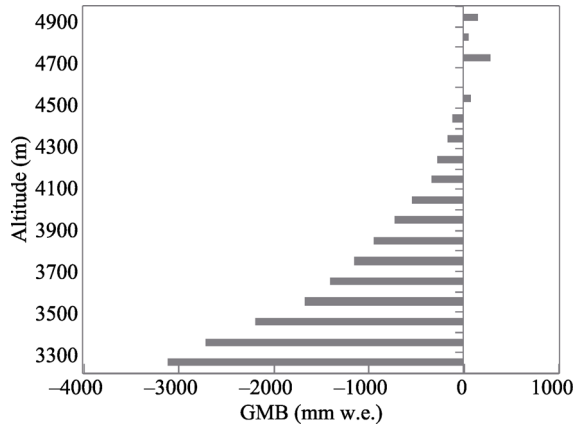

Figure 4 The values for the GMB in each elevation zone in the Manas River Basin

To examine how the GMB varied with increase of altitude, a linear regression model for the ablation area, the accumulation area and the overall glacier was built (Table 5), based on a slow accumulation rate of 18.77 mm w.e./100 m in the accumulation area (R^2 = 0.073) and a rapid ablation rate of –244.83 mm w.e./100 m in the ablation area (R^2 = 0.93). As to the whole glacier, there was clear correlation between the GMB and altitude with a linear rate of increase of 179.09 mm w.e./100 m (R^2 = 0.87). This relationship suggests that overall the glacier underwent ablation in the MRB. Furthermore, the performance behavior of the glacier in terms of the variation of the GMB with altitude was not a simple linear increase but constantly tended towards the ELA (R^2 = 0.993), because the rise of altitude mainly impacted the GMB through changing the vertical distribution of water and heat to achieve a new balance. Besides, the variation of the degree-day factors, the slope, the aspect and the wind also affected the performance of the GMB. Affected by these basic elements, the vertical change of the GMB in the MRB initially exhibited a growth trend and then decreased slowly (Figure 4).

Table 5 Variation of the fitting curves of the GMB with altitude in the glacier zones

Region	Fitting equation	Correlation
Ablation area	y1 = 2.4483x – 10729	R^2 = 0.927
Accumulation area	y2 = 0.1877x – 788.3	R^2 = 0.073
Glacier region (whole)	y3 = 1.7909x – 2522.5 (linear)	R^2 = 0.873
	y4 = $–0.0014x^2$ +13.75x – 32691 (non-linear)	R^2 = 0.993

Note: y1, y2, y3 and y4 represent the GMB in each area; x represents altitude.

4.3 Factors influencing the GMB

Glacier meltwater, produced by the changes of the GMB, has an evident replenishment effect on river runoff in arid areas. The intraannual changes of the GMB to runoff indicate that the strongest glacier melting (–575.63 mm w.e.) accounted for 75.4% of the total annual amount of the GMB in July and August, while the runoff (7.73×10^8 m^3) accounted for 55.1% of the total annual amount of runoff and also reached an annual peak (Figure 3b). Though there was a strong monthly correlation between the GMB and runoff, their peak periods were not quite coincident. The peak for the GMB occurred in August but the peak for the runoff was in July, reflecting the fact that the annual maximum precipitation supplied runoff in July when precipitation had a mitigating effect on glacier melting such as to weaken the glacier loss. However, the whole glacier was melting in August when the temperature had risen and precipitation fell in liquid form on the glacier surface, which resulted in more melting. Thus it is concluded that the interannual synergism of runoff to the monthly GMB reflects the good replenishment effect of the glacial "solid reservoir."

Most inland rivers in alpine mountains originate from the "three-elements" (glacier meltwater, rainfall and snow) and they are all crucial replenishment sources for river runoff. During the study period, the interannual recharge rates of glacier meltwater varied from 19% to 31% (average value 25%), which shows a rising upward trend of glacier ablation with intensified glacier melting. The interannual synchronicity shows that the overall correlation coefficient between runoff and the GMB was –0.49. The key point is that the GMB greatly altered replenishment to runoff around 2009 given that the correlation coefficient was reduced from –0.58 to –0.45, while the correlation coefficient between the glacier meltwater and the runoff was reduced from 0.40 to 0.38, which implies that the regulation for the GMB to runoff was weakened. Investigations (Zheng, 2018) on the evolution of runoff in the MRB indicated that climate warming and humidification have become more evident since 2009, and this would have a strong impact on river runoff in alpine mountains. The runoff is highly dependent on climate change, as rising temperatures would cause an acceleration of the melting of snow and increased precipitation, which together would enhance the contributions of precipitation and snow meltwater to runoff.

5 Discussion

5.1 Effects of the degree-day factors

The degree-day factors which play a decisive role in the GMB change include the snow degree-day factor (D_s) and the ice degree-day factor (D_i). It seems that D_s shows a rapid decrease at the extremes but a gradual rise in the middle whereas D_i shows a decrease at the beginning and then rises gradually (Figure 5); the maximum for the D_s (2.60 mm/(℃·d)) was at the glacial terminal while the minimum (2.21 mm/(℃·d)) was at the top of the glacier, with an average value of 2.44 mm/(℃·d). Chen *et al*. (2015) considered that the distinct moisture content of the snow layer causes a spatial dispersion of snow density which further affects the D_s value. At low altitudes, snow melts rapidly under the influence of strong solar radiation thus the snow layer has more moisture content of a higher density, while at higher altitudes, snowcover has less moisture content of lower density under the weaker solar

radiation. Although solid precipitation increases from the terminal to the top of glacier, which also makes the snow density become larger, the impact of this densification process on snow density is relatively weak, compared to the impact caused by changes in the moisture content. Besides, the transformation of the D_s above 3900 m may be induced by the action of wind. The volume at the top of glacier is persistently decreasing under wind action, which brings about snow accumulation that makes the D_s become larger under densification at altitudes of 3900–4700 m. As for the D_i, it originally decreased from the glacial terminal to 4100 m and then increased vertically from 4100 m to the glacial top, ranging from 2.75 to 4.78 mm/(℃·d) with an average value of 3.70 mm/(℃·d), while the minimum occurred around 4100 m and the maximum was at the top of the glacier. Zhang *et al*. (2006) thought that the vertical variation of the D_i is related to the glacial terrain conditions such as elevation, slope, aspect, shelter, moraine coverage and local climate. If the glacial surface topography is more favorable to receiving solar radiation or the climate becomes warmer and wetter, the glacier will melt more readily and the Di will become larger. Therefore, the minimum of the D_i occurred at 4100 m where the stronger solar radiation or the drier cold climate or the greater sublimation may inhibit glacier ablation. The values of the D_s and D_i can encompass the melting ability of the glacier. Although solar radiation is the most direct factor to affect the D_s and D_i, terrain conditions can still influence the absorption of solar radiation in addition to meteorological elements such as the relative humidity and wind which can also impact on the D_s and D_i.

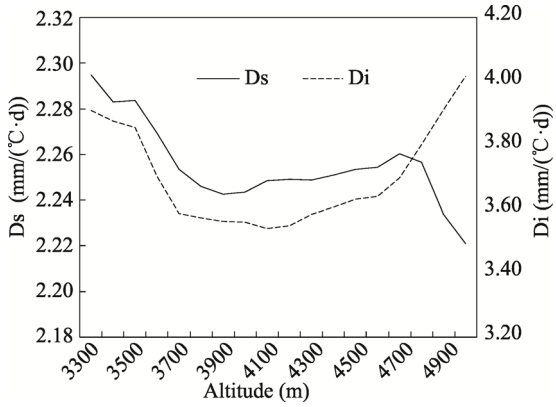

Figure 5 Changes for the ice and snow degree-day factors in the Manas River Basin

5.2 Spatial distribution of the GMB and recharge rates of glacier meltwater to runoff

To explore the distribution patterns of GMB in the Tianshan Mountains, the values for the GMB in the MRB for the east and west branches of Glacier No.1 and Glacier No.51 were compared for the same period. Zhang *et al.* (2018) simulated the GMB of Glacier No.51 where it reached –370 mm w.e./a from 1999 to 2015. Also Zhang (2014) used the measured data to conclude that the GMB was –582 mm w.e./a in the west branch and –485 mm w.e./a in the east branch of Glacier No.1 from 1990 to 2010. In the corresponding periods, the GMB of the MRB was –577.13 mm w.e./a. By comparing the GMB values for the above glaciers, it was revealed that the glacial negative state was intensified from west to east in the Tianshan Mountains at that time. Zhang *et al*. (2018) surmised that the primary reason for differences in the GMB values in the above glaciers was the influence of westerly winds, especially during the glacier melting period, while precipitation declined from the west to the east so that the spatial distribution of the GMB decreased from the west to the east in the Tianshan Mountains. Moreover, the spatial distribution of the GMB was also restricted by the diverse topographies and geomorphologies, which made the GMB vary locally given the different values in the east and the west branches of Glacier No.1. In general, to comprehen-

sively analyze the spatial distribution of the GMB, attention should be paid not only to the direct effects of climate change, but, also, differences caused by indirect factors such as topography should be taken into account.

Glacier meltwater plays a decisive role in regulation and replenishment of rivers and there are clear differences on recharge rates of glacier meltwater to runoff in arid basins. During the study period, the annual recharge rates of glacier meltwater to runoff fluctuated between 19% and 31% in the MRB, while recharge rates ranged from 32.8%–38.5% in the Tarim Inner-flow Basin, 12.01%–11.4% in the Turpan-Hami endorheic drainage and 16.9%–13.7% in the Yili River Basin (Yang, 1987; Shen *et al*., 2013). As the production of the glacier changes, the distinct spatial distribution of recharge rates reflects the fact that if the negative GMB is further enhanced or the glacier area dramatically retreats, the glacier melting will be stronger and the recharge rate will rise continuously, otherwise, it will decrease. Moreover, the recharge rate is also affected by precipitation and snow meltwater outside of the glacier. The recharge rate of glacier meltwater to runoff is 27.1% in the Junggar endorheic drainage area, 29.4% in the Kuytun River Basin (Shen *et al*., 2013), 34.6% in the MRB (Yang, 1987), 26.7% in the Urumqi River Basin (Sun *et al*., 2017) and 37.6% in the Baiyang River Basin (Li *et al*., 2011), reflecting an overall upward trend from the west to the east in the Tianshan Mountains, however, the upward trend is not simply rising but actually fluctuating. Given that the negative value of the GMB continues to rise from the west to the east in the Tianshan Mountains, it is concluded that the recharge rate of glacier meltwater to runoff is not only affected by the GMB change but also by precipitation and snow meltwater from outside of the glacier.

6 Conclusions

(1) Based on the multi-source remote sensing data, inversion models of temperature and precipitation in the Tianshan Mountains were established. Using downscaling methods, the vertical characteristics of temperature and precipitation in the MRB were analyzed. It was shown that the lapse rate of temperature was –0.57℃/100 m and –0.03℃/100 m below and above 4200 m, respectively, while the precipitation gradient was 4.89 mm/100 m below 4200 m, 2.66 mm/100 m from 4200 m to 4700 m and 5.17 mm/100 m above 4700 m, respectively; besides the maximum precipitation zone lay at altitudes between 4100 m and 4200 m. Based on the analysis, the inversion of remote sensing meteorological data can faithfully depict the spatial distribution details of temperature and precipitation in an alpine glacier area.

(2) Multi-source remote sensing data were used to drive the degree-day model to simulate the GMB in the MRB. During the study period, the interannual changes of the GMB maintained continuous negative states while the annual GMB varied from –464.85 mm w.e./a to –632.19 mm w.e./a and the cumulative GMB was up to –9811.19 mm w.e., with the ELA varying from 4057 m to 4588 m. Besides, the glacier melting slowed down during 2000–2002 and 2008–2010 but intensified for 2002–2008 and 2010–2016, while the strongest glacier ablation was during 2005–2009. However, the intraannual changes of the GMB showed that the strongest glacier accumulation occurred in April when precipitation had clearly increased, but the strongest glacier ablation occurred in August when the temperature rose dramatically.

(3) During the study period, river runoff responded strongly to change of the GMB. The most serious intraannual GMB loss reached –575.63 mm w.e. in July and August, accounting for 75.4% of the annual change, which made the runoff account for 55.1% of the annual GMB loss. Besides, the interannual glacier meltwater fluctuated between 19% and 31%, which may have been caused by the differences in precipitation and snow meltwater outside of the glaciers in the MRB.

Above all, there was a small constraint deficiency in the defaults for multi-period glacier area data, so that the changes of glacier area in calculating the GMB were somewhat compromised. As some researchers have indicated, ignoring the changes of area of the glacier would lead to a certain deviation in the GMB estimation, especially for the current global climate warming scenario, which may overestimate the loss of the GMB (Wang *et al.*, 2011). Thus we aim to clarify the effect of different glacier areas on changes of the GMB in future studies.

References

Cao Y Q, Zhang W, Wang W J *et al.*, 2018. Evaluation of TRMM 3B43 data over the Yangtze River Delta of China. *Scientific Reports*, 8(1): 5290–5290.

Cascone S, Coma J, Gagliano A *et al.*, 2019. The evapotranspiration process in green roofs: A review. *Building and Environment*, 147: 337–355.

Chen N, Feng X Z, Xiao P F *et al.*, 2015. Analysis of snow layer parameters in Manasi River Basin. *Journal of Nanjing University* (*Natural Sciences*), 51(5): 936–943. (in Chinese)

Chen R S, 2014. Some knowledge on and parameters of China's alpine hydrology. *Advances in Water Science*, 25(3): 307–317. (in Chinese)

Ezzine H, Bouziane A, Ouazar D *et al*., 2017. Downscaling of open coarse precipitation data through spatial and statistical analysis, integrating NDVI, NDWI, elevation, and distance from sea. *Advances in Meteorology*, 99(8): 1–20.

Jia S F, Zhu W B, Lu A F *et al.*, 2011. A statistical spatial downscaling algorithm of TRMM precipitation based on NDVI and DEM in the Qaidam Basin of China. *Remote Sensing of Environment*, 115(12): 3069–3079.

Kronenberg M, Barandun M, Hoelzle M *et al.*, 2016. Mass-balance reconstruction for Glacier No.354, Tien Shan, from 2003 to 2014. *Annals of Glaciology*, 57(71): 92–102.

Lan Y C, Shen Y P, Wu S F *et al.*, 2007. Changes of the glaciers and the glacier water resources in the typical river basins on the north and south slopes of the Tianshan Mountains since 1960s. *Journal of Arid Land Resources and Environment*, 21(11): 1–8. (in Chinese)

Li B F, Chen Y N, Chen Z S *et al.*, 2012. Trends in runoff versus climate change in typical rivers in the arid region of northwest China. *Quaternary International*, 282(19): 87–95.

Li K M, Li Z Q, Gao W Y, 2011. Recent retreat of glaciers in the East Tianshan Mountains of Xinjiang and its impact on water resources. *Chinese Science Bulletin*, 56(32): 2708–2716.

Li Y, Tao H, Su B D *et al.*, 2019. Impacts of 1.5°C and 2°C global warming on winter snow depth in Central Asia. *Science of The Total Environment*, 651(15): 2866–2873.

Mackay J D, Barrand N E, Hannah D M *et al.*, 2018. Glacio-hydrological melt and runoff modelling: Application of a limits of acceptability framework for model comparison and selection. *The Cryosphere*, 12(7): 2175–2210.

Mcpartland M Y, Kane E S, Falkowski M J *et al.*, 2019. The response of boreal peatland community composition and NDVI to hydrologic change, warming and elevated carbon dioxide. *Global Change Biology*, 25(1): 93–107.

Michaelides S, Karacostas T, Sanchez J L *et al.*, 2017. Reviews and perspectives of high impact atmospheric processes in the Mediterranean. *Atmospheric Research*, 208(1): 4–44.

Mu J X, Li Z Q, Zhang H *et al.*, 2019. Mass balance variation of continental glacier and temperate glacier and their response to climate change in western China: Taking Urumqi Glacier No.1 and Parlung No.94 Glacier as examples. *Arid Land Geography*, 42(1): 20–28. (in Chinese)

Muattar S, Ding J L, Abudu S *et al.*, 2016. Simulation of snowmelt runoff in the catchments on northern slope of

the Tianshan Mountains. *Arid Zone Research*, 33(3): 636–642. (in Chinese)

Naegeli K, Huss M, Hoelzle M, 2019. Change detection of bare-ice albedo in the Swiss Alps. *The Cryosphere*, 13(1): 397–412.

Shen Y P, Su H C, Wang G Y *et al.*, 2013. The responses of glaciers and snow cover to climate change in Xinjiang (I): Hydrological effects. *Journal of Glaciology and Geocryology*, 35(3): 513–527. (in Chinese)

Shi Y F, 2009. Concise Glacier Inventory of China. Shanghai: Shanghai Popular Science Press. (in Chinese)

Smid M, Costa A C, 2018. Climate projections and downscaling techniques: A discussion for impact studies in urban systems. *The International Journal of Urban Sciences*, 22(3): 277–307.

Song C Q, Huang B, Ke L H *et al.*, 2016. Precipitation variability in High Mountain Asia from multiple datasets and implication for water balance analysis in large lake basins. *Global and Planetary Change*, 145(5): 20–29.

Sun C J, Chen W, 2017. Streamflow components in inland rivers in the Tianshan Mountains, Northwest China. *Arid Land Geography*, 40(1): 37–44.

Van D B M R, Bus C, Ettema J *et al.*, 2010. Temperature thresholds for degree-day modelling of Greenland ice sheet melt rates. *Geophysical Research Letters*, 37(18): 1–5.

Wang G Y, Shen Y P, 2011. The effect of change in glacierized area on the calculation of mass balance in the Glacier No.1 at the Headwaters of Urumqi River. *Journal of Glacilogy and Geocryology*, 33(1): 1–7. (in Chinese)

Wang P Y, Li Z Q, Li H L *et al.*, 2016. Recent evolution in extent, thickness, and velocity of Haxilegen Glacier No.51, Kuytun River Basin, Eastern Tianshan Mountains. *Arctic*, *Antarctic*, *and Alpine Research*, 48(2): 241–252.

Wang X, Yang T, Xu C *et al.*, 2019. Understanding the discharge regime of a glacierized alpine catchment in the Tianshan Mountains using an improved HBV-D hydrological model. *Global and Planetary Change*, 172(17): 211–222.

Wang X C, Dong X B, Liu H M *et al.*, 2017. Linking land use change, ecosystem services and human well-being: A case study of the Manas River Basin of Xinjiang, China. *Ecosystem services*, 27(13): 113–123.

Wu L H, Li H L, Wang L, 2011. Application of a degree-day model for determination of mass balance of Urumqi Glacier No.1, Eastern Tianshan, China. *Journal of Earth Science*, 22(4): 470–481.

Xu Z H, Fan W G, Wei H J *et al.*, 2019. Evaluation and simulation of the impact of land use change on ecosystem services based on a carbon flow model: A case study of the Manas River Basin of Xinjiang, China. *Science of The Total Environment*, 652(206): 117–133.

Yang Z N, 1987. Glacier water resources in China. *Natural Resources*, 9(1): 46–55. (in Chinese)

Zhang G, Li Z, Wang W *et al.*, 2013. Mass balance change in east and west branches of Glacier No.1 at Urumqi riverhead, China, during last 20 years. *Chinese Journal of Ecology*, 32(9): 2412–2417. (in Chinese)

Zhang G F, 2014. Glacier matter balance and its relation to climate change at the source of Urumqi River, Tianshan, China [D]. Lanzhou: Northwest Normal University. (in Chinese)

Zhang H, Li Z Q, Zhou P *et al.*, 2018. Mass-balance observations and reconstruction for Haxilegen Glacier No.51, eastern Tien Shan, from 1999 to 2015. *Journal of Glaciology*, 64(247): 689–699.

Zhang Q, Shi P J, Singh V P *et al.*, 2017. Spatial downscaling of TRMM-based precipitation data using vegetative response in Xinjiang, China. *International Journal of Climatology*, 37(10): 3895–3909.

Zhang R B, Wei W S, Shang H M *et al.*, 2019. A tree ring-based record of annual mass balance changes for the TS. Tuyuksuyskiy Glacier and its linkages to climate change in the Tianshan Mountains. *Quaternary Science Reviews*, 205(28): 10–21.

Zhang S Q, Ye B S, Liu S Y *et al.*, 2012. A modified monthly degree-day model for evaluating glacier runoff changes in China. Part I: Model development. *Hydrological Processes*, 26(11): 1686–1696.

Zhang T, Li B L, Yuan Y C *et al.*, 2018. Spatial downscaling of TRMM precipitation data considering the impacts of macro-geographical factors and local elevation in the Three-River Headwaters Region. *Remote Sensing of Environment*, 215(4): 109–127.

Zhang Y, Liu S Y, Xie C W *et al.*, 2006. Application of a degree-day model for the determination of contributions to glacier meltwater and runoff near Keqicar Baqi glacier, southwestern Tien Shan. *Annals of Glaciology*, 43(180): 280–284.

Zheng J T, 2018. Research on runoff evolution in mountainous area under climate change in Manas River [D]. Shihezi: Shihezi University. (in Chinese)

Zhu G F, Qin D H, Liu Y F *et al.*, 2017. Accuracy of TRMM precipitation data in the southwest monsoon region of China. *Theoretical and Applied Climatology*, 129(7): 1–10.